The Cryosphere Discuss., 6, 4137–4169, 2012
www.the-cryosphere-discuss.net/6/4137/2012/
doi:10.5194/tcd-6-4137-2012

The Cryosphere Discussions

Changes in seasonal snow liquid water content during the snowmelt period in the Western Tianshan Mountains, China

H. Lu[1,2], W. S. Wei[3], M. Z. Liu[1,4], X. Han[3], and W. Hong[1,2]

[1]Xinjiang Institute of Ecology and Geography, Chinese Academy of Sciences, Urumqi 830011, China
[2]University of Chinese Academy of Sciences, Beijing 100049, China
[3]Institute of Desert Meteorology, CMA, Urumqi 830002, China
[4]Tianshan Station for snow & Avalanche Research, Urumqi 830011, China

Received: 10 August 2012 – Accepted: 10 September 2012 – Published: 27 September 2012

Correspondence to: H. Lu (luhengwzs@163.com)

Published by Copernicus Publications on behalf of the European Geosciences Union.

Abstract

Snow liquid water content is a very important parameter for snow hydrological processes, avalanche research and snow cover mapping by remote sensing. Snow liquid water content was measured with a portable instrument (Snow Fork) in the Tianshan Station for Snow Cover and Avalanche Research, Chinese Academy of Sciences during the snowmelt period in spring 2010. This study analyzed the temporal and spatial distribution of snow liquid water content in different weather conditions. The average liquid water content of snow in the whole layer exponentially increased and can be calculated using a regression function of prior moving average temperature. The proportion of net radiation, sensible heat flux and latent heat flux in total energy changed in different snowmelt period. During the pre-snowmelt period ($0.3\,\% \leq W_{vol} < 1\,\%$), snow liquid water content and its temporal variation were relatively small, with liquid water accumulated in the coarse snow layer. During the mid-snowmelt period ($1\,\% \leq W_{vol} < 2.5\,\%$), the variation was significant in the upper layer and decreased drastically during the snowfall and the following one to two days. Only the temporal variation decreased after rain or snow (ROS) events. During the late-snowmelt period ($W_{vol} \geq 2.5\,\%$), the distribution and variation of every snow layer showed a uniform trend, and the effect of ROS events on liquid water content only occurred during rainfall and snowfall.

1 Introduction

Snow cover can be either dry or wet snow. Dry snow is a mixture of snow crystals and air, whereas wet snow is a combination of snow crystals, air, and liquid water. Liquid water may come from rainfall or snowmelt. In the absence of rainfall, liquid water comes from snowmelt generated by air temperature and solar radiation. Snow liquid (or free) water content is a very important parameter for thermal conductivity (Singh, 1999), metamorphism (Wakahama, 1956; Colbeck, 1987; Marsh, 1987), hardness (Lzumi, 1989; Trautman et al., 2006), avalanche (Brun et al., 1989; Conway et al., 1993; Mitterer et al., 2009), snowmelt (Jones et al., 1983), and reservoir management (Kattelmann et al., 1999). Snow liquid water content was previously recognized as a quantifiable parameter of hydrologic significance. However, it was not used regularly as a snowpack characteristic because of difficulties in field measurements. Various techniques have been used or proposed to measure snow liquid water content. Some of these techniques include centrifugal separation (Jones, 1979), freezing-point depression (Morris, 1981), freezing calorimetry (Jones et al., 1983; Boyne et al., 1987), melting calorimetry (Kawashima et al., 1998), alcohol calorimetry (Fisk, 1986), dilution (Davis et al., 1985; Boyne et al., 1987), and dielectric constant measurement (Boyne et al., 1987; Denoth, 1994; Schneebeli et al., 1998). Point observations of snow liquid water content have been conducted using these methods. Remote sensing technology approaches could be employed to measure snow liquid water content in the superficial layer across a large area (Dozie et al., 2004). Liquid water content could be estimated using hand test and dielectric methods. Techel et al. (2010) compared these two methods using Snow Fork and Denoth wetness instrument in the Swiss Alps, mostly above tree line.

Combined with snow temperature variation, snow liquid water content was used as an indicator to divide the stable period ($W_{vol} < 0.1\,\%$), interim period ($0.1\,\% < W_{vol} < 0.3\,\%$), and snowmelt period of seasonal snow ($W_{vol} > 0.3\,\%$) in the Western Tianshan Mountains (Chen et al., 2012). Zhang et al. (1986) and Wei et al. (2001) demonstrated that low temperature is the primary factor for the small snow liquid water content across the northwestern region of China. Techel et al. (2010) investigated the reliability of point observations in relation to temporal and small-scale spatial variability. Their results showed that slope aspect slope inclination, elevation, and distance to the rocky area are important factors for snow liquid water. Li et al. (2007) evaluated snow liquid water content, determined the relationship between liquid water content and snow temperature, and identified the temporal and spatial distribution of liquid water content in the Arctic using a set up with known physical parameters of snow and ice. Che et al. (2008) demonstrated the changes in liquid water content with temperature and time. Using the freezing calorimetry method, Jones et al. (1983) observed the daily changes in snowpack liquid water content determined by three different operators in Fraser, Colorado. Niang et al. (2006) simulated the characteristics of snowpack density and liquid water content using Looyenga's mixing coefficient model. Colbeck (1972, 1982), Lehua Pan et al. (1997), and Zhou et al. (2001) simulated surface snow melting and water percolation for several days. This study aims to analyze the temporal and spatial changes in snow liquid water content during the snowmelt period in the Western Tianshan Mountains in China using Snow Fork. The mechanism by which different weather conditions affect snow liquid water content is also analyzed. The results of this study provide basic data for further studies on snow characteristics and snow cover hydrological processes.

2 Method and data

2.1 Study area

The study was conducted at the Tianshan Station for Snow Cover and Avalanche Research, Chinese Academy of Sciences (TS), which is located at 43°16′ N, 84°24′ E at an elevation of 1776 m a.s.l. The station lies in the upper reaches of the Künes River in the central zone of the Western Tianshan Mountains, China. Seasonal snow in TS lasts from late October to early April, with a mean annual depth of 0.78 m. The maximum depth has not exceeded 1.6 m since 1967. Snow in this region is of dry-cold type, with low density and low snow liquid water content by volume, and depth hoar develops largely compared with other places in China (Wei et al., 2001). The study area is a 25 m × 25 m grass-covered area in the observation field. Data of meteorology, density, water content, permittivity, and other factors were collected in different snow layers from 3 March 2010 to 26 April 2011 during the snow cover period. Morning liquid water content (before sunrise) was mainly affected by the meteorological condition from prior night to this morning. Thus, the period of last 20:00 to this 20:00 LT was estimated as one day in this study.

2.2 Snow liquid water content and snow density

A column of snow was dug out to allow for the measurement of the vertical snow profile. To avoid lateral impact by solar radiation on subsequent vertical snow profiles, the position of each succeeding snow column was dug out by at least 0.3 m from the previous column. The measurements were conducted at every 2 cm depth from the surface to the bottom using a Finnish Snow Fork gauge (model LK, Ins. Toimisto Toikka Oy, Espoo, Finland). Seven parameters (attenuation rate, resonance frequency, 3 dB band width, relative dielectric constant, volumetric moisture, density, and weighted water content) were obtained using the Snow Fork gauge (Sihvola et al., 1986). According to the instruction of Snow Fork gauge, the mathematical principle for the calculation of snow density and liquid water content by volume is expressed as follows:

$$W_{\mathrm{vol}} = -0.06 + \sqrt{0.06^2 + \epsilon''/(0.0075 \cdot f)} \tag{1}$$

$$\rho = -1.2142857 + \sqrt{1.2142857^2 - (1 + 8.7 \cdot W_{\mathrm{vol}} + 70 \cdot W_{\mathrm{vol}}^2 - \epsilon')/0.7 + W_{\mathrm{vol}}} \tag{2}$$

where W_{vol} is the snow liquid water content by volume (%), ρ is the snow density (g cm^{-3}), f is the frequency, ϵ' is the real part of relative permittivity, and ϵ'' is the imaginary part of relative permittivity.

The liquid water content was measured before sunrise (08:00) and after sunset (20:00). The afternoon liquid water content was estimated as the daily value in this paper because of the occasional absence of measurement before sunrise.

2.3 Air temperature

A single-channel automatic temperature recorder (RC-30, Jingchuang Electrics Co., Ltd, Shanghai) was used to measure the air temperature. The temperature was calculated by measuring the resistance of a platinum resistance thermister, with a precision of ±0.1 °C. The time interval of the recorder was set to 5 min and its probe was mounted in an instrument shelter 150 cm above the ground, which was the standard height for thermometer installation. After eliminating the obvious false data, air temperature indices of daily average, maximum, minimum and accumulated air temperature were statistically calculated. The accumulated air temperature is the summation of the hourly average air temperature higher than 0 °C, with an accuracy of ±2.4 °C (±0.1 × 24 = 2.4 °C).

$$T_{ac} = \sum_{i=1}^{23} T_i, \quad T_i \geq 0 \tag{3}$$

where T_{ac} is the accumulated air temperature (°C), T_i is the hourly average air temperature higher than 0 °C.

2.4 Surface energy balance

The snow surface energy balance equation is expressed as (Jin et al., 1999):

$$Q_m = K + L + H + L_V E + I_{prec} + G \tag{4}$$

where Q_m is the total energy (MJ m^{-2}), K is the net shortwave radiation (MJ m^{-2}), L is the net longwave radiation (MJ m^{-2}), H is the sensible heat flux (MJ m^{-2}), $L_V E$ is the latent heat flux (MJ m^{-2}), I_{prec} is the energy supplied by precipitation (heat flux advected to the snowpack by rain or snow) (MJ m^{-2}), and G is the ground heat flux (not considered in this study). Radiation was measured using pyrgeometers (EKO Instruments Co., Ltd. with a precision of ±2.5 %).

Daily sensible (H) was calculated as a function of the temperature gradient above the snow surface (Boon, 2009):

$$H = \rho_a C_{pa} D_H (T_a - T_{ss}) \tag{5}$$

TCD
6, 4137–4169, 2012
Changes in snow liquid water
H. Lu et al.
Title Page | Abstract | Introduction | Conclusions | References | Tables | Figures | Back | Close | Full Screen / Esc | Printer-friendly Version | Interactive Discussion
Discussion Paper | Discussion Paper | Discussion Paper | Discussion Paper

where ρ_a is the density of air ($kg\,m^{-3}$), C_{pa} is the heat capacity of air ($J\,kg^{-1}\,K^{-1}$), and D_H is the bulk transfer coefficient for sensible heat ($m\,s^{-1}$).

Daily latent heat flux ($L_V E$) was calculated as a function of the vapor pressure gradient above the snow surface (Boon, 2009):

$$L_V E = \rho_a \lambda_V D_E \frac{0.622}{P}(e_a - e_{ss}) \quad (6)$$

where λ_V is the latent heat of vaporization ($2.48 \times 10^6\,J\,kg^{-1}$), D_E is the bulk transfer coefficient for latent heat ($m\,s^{-1}$), P is the atmospheric pressure (kPa), and e_a and e_{ss} are the atmospheric and snow surface vapor pressure (kPa), respectively.

Under neutral atmospheric conditions, $D_H = D_E$ (Anderson, 1976; Male and Gray, 1981)

$$D_H = D_E = \frac{k^2 u_a}{\left[\ln\left(\frac{z_a}{z_0}\right)\right]^2} \quad (7)$$

where k is von Karman's constant (0.40), u_a is the wind speed ($m\,s^{-1}$), z_a is the wind height of the wind measurement (m), and z_0 is the roughness length of the snow surface (m). Values of z_0 from the literature range from 0.0002 to 0.02 m (Moore, 1983). Because of the absence of field-based z_0 measurements, the value of z_0 is equal to 0.06 m according to Boon's study (Boon, 2009).

The bulk aerodynamic method (Richardson number) was used to correct the turbulent fluxes under highly stratified conditions:

$$Ri = \frac{g(T_a - T_{ss})z_a}{u_a^2 T_K} \quad (8)$$

where g is the gravitational acceleration ($m\,s^{-1}$) and T_K is the mean temperature of air layer (K). Ri was positive for the duration of each ablation period. Thus, turbulent flux calculations were corrected only for damping of turbulence under stable atmospheric conditions ($Ri > 0.3$, Andreas, 2002) using the following equation (Moore, 1983; Boon, 2009), where $D_M = D_H = D_E$:

$$D_{Mc} = D_M/(1 + 10Ri) \tag{9}$$

Energy supplied by precipitation (I_{prec}) was calculated using the following equation (Jin et al., 1999):

$$I_{prec} = \begin{cases} C_l p_0 (T_P - 273.15) & \text{(for rainfall)} \\ C_V \frac{P_0 f_{ice}}{\gamma_i} (T_P - 273.15) - P_0 L_{li} & \text{(for snowfall)} \end{cases} \tag{10}$$

where C_l is the specific heat of water ($4217.7\,\mathrm{J\,kg^{-1}\,K^{-1}}$), p_0 is the effective rate of precipitation on land surface ($\mathrm{kg\,m^{-2}\,s^{-1}}$), C_V is the volumetric specific heat capacity of snow ($\mathrm{J\,kg^{-1}\,K^{-1}}$), T_P is the precipitation temperature (K), $T_P = T_a$, L_{li} is the heat of fusion ($\mathrm{J\,kg^{-1}}$), f_{ice} is the ice mass fraction of precipitation, and γ_i is the partial density of ice in snowfall ($\mathrm{kg\,m^{-3}}$).

Volumetric specific heat capacity of snow was calculated using the following equation (Verseghy, 1991):

$$C_V = 1.9 \times 10^6 \frac{\rho_S}{\rho_i} \tag{11}$$

where ρ_S is the snow density ($\mathrm{kg\,m^{-3}}$) and ρ_i is the ice density ($917\,\mathrm{kg\,m^{-3}}$).

Ice mass fraction of precipitation (f_{ice}) was calculated using the following equation (Jin et al., 1999):

$$f_{ice} = \begin{cases} 0.0 & T_a > 2.5\,^\circ\mathrm{C} \\ 0.6 & 2.0\,^\circ\mathrm{C} < T_a \leq 2.5\,^\circ\mathrm{C} \\ 1 - [54.62 - 0.2(T_a + 273.15)] & 0.0\,^\circ\mathrm{C} < T_a \leq 2.0\,^\circ\mathrm{C} \\ 1.0 & T_a \leq 0^\circ \end{cases} \tag{12}$$

TCD
6, 4137–4169, 2012

The partial density of ice in snowfall (γ_i) was calculated using the following equation (LaChapelle, 1969):

$$\gamma_i = \begin{cases} 0.0 & T_a > 2.5\,^\circ\mathrm{C} \\ 189.0 & 2.0\,^\circ\mathrm{C} < T_a \leq 2.5\,^\circ\mathrm{C} \\ 50.0 + 1.7(T_a + 14.99)^{1.5} & -15\,^\circ\mathrm{C} < T_a \leq 2.0\,^\circ\mathrm{C} \\ 50.0 & T_a \leq -15\,^\circ\mathrm{C} \end{cases} \quad (13)$$

2.5 Snow liquid water-holding capacity

The liquid water movement in the snowpack is not dynamically described. When liquid water content in a snow layer exceeds the liquid water-holding capacity, the excess water flows to the underlying layer. Liquid water content (C^R) was calculated using the following equation (Anderson, 1976):

$$C^R = \begin{cases} C^R_{\mathrm{min}} & \gamma_i \geq \gamma_e \\ C^R_{\mathrm{min}} + \left(C^R_{\mathrm{max}} - C^R_{\mathrm{min}}\right) \frac{\gamma_e - \gamma_i}{\gamma_e} & \gamma_i < \gamma_e \end{cases} \quad (14)$$

where $C^R_{\mathrm{min}} = 0.03$, $C^R_{\mathrm{max}} = 0.1$, $\gamma_e = 200\,\mathrm{kg\,m^{-3}}$, and $\gamma_i = \rho_S f_{\mathrm{ice}}$ is the partial density of ice ($\mathrm{kg\,m^{-3}}$). f_{ice} is the ice mass fraction of snow and can be calculated using the following equation:

$$f_{\mathrm{ice}} = 1 - \frac{W_{\mathrm{vol}}}{\rho_S} \quad (15)$$

where W_{vol} is the snow liquid water content (%) and ρ_S is the snow density ($\mathrm{g\,cm^{-3}}$).

TCD
6, 4137–4169, 2012

Title Page
Abstract | Introduction
Conclusions | References
Tables | Figures
◀| |▶
◀ ▶
Back | Close
Full Screen / Esc
Printer-friendly Version
Interactive Discussion

3 Results and discussion

3.1 Temporal changes in snow liquid water content during the snowmelt period

The average liquid water content in the whole snow layer exponentially increased (Fig. 1). The changes in melt rates were consistent with those in liquid water content. Water content ranged from 0.39 % to 8.35 %, with a density range of 0.22 $g\,cm^{-3}$ to 0.44 $g\,cm^{-3}$. From 3 March to 14 March, liquid water content was less than 1 %, with a range of 0.39 % to 0.94 % and an average of 0.54 %. From 16 March to 13 April, liquid water content ranged from 1 % to 2.5 % (2.08 % on average), and snowpack outflow was observed. After 14 April, liquid water content was higher than 2.5 %, with an average of 5.41 %. Liquid water content sharply increased to 0.54 $\%\,d^{-1}$, and the melt rate in this period was 2.6 times greater than that between 16 March and 13 April. Given the changes in liquid water content in the whole snow layer, the snowmelt period can be divided into three stages (pre-snowmelt period: $0.3\,\% \le W_{vol} < 1\,\%$, mid-snowmelt period: $1\,\% \le W_{vol} < 2.5\,\%$, and late-snowmelt period: $W_{vol} \ge 2.5\,\%$).

Snowpack condition is significantly affected by air temperature. Snow liquid water content showed a significant and positive correlation with the daily average, maximum, minimum, and accumulated air temperature (Table 1). The correlation coefficient between accumulated air temperature and liquid water content was higher than that between average air temperature and liquid water content. The average water content of the whole layer exponentially increased with the average air temperature and linearly increased with accumulated air temperature (Fig. 2). However, the liquid water content scattered widely, suggesting that the different temperature indices could only indicate the energy balance of snow surface to a certain extent. The wide scattering of liquid water content was partly caused by the mass balance of snowpack.

Figure 3 shows the daily heat flux input during the snowmelt period, including shortwave radiation, longwave radiation, net radiation, sensible heat flux and latent flux. Snow liquid water content exponentially increased during the snowmelt period, with net radiation and sensible heat flux dominating, and latent heat flux taking a small proportion. Both net radiation and sensible heat flux were generally positive during the snowmelt period, which contributed to 48.3 % and 27.3 % of the total energy (not including energy supplied by precipitation). The proportion of net radiation increased drastically from the pre-snowmelt period to the late-snowmelt period. This result can be attributed to the increase in astronomical radiation with time and the changes in snow surface albedo. During the pre-snowmelt period, air temperature increased and became higher than snow surface temperature, especially during daytime. The high air temperature and the lower air humidity caused the sensible heat flux to become the most important part of total energy. Specific humidity during the mid-snowmelt period increased and became 1.08 $\mathrm{g\,g^{-1}}$ higher than that during the pre-snowmelt period. Therefore, the proportion of latent heat flux is higher than that of sensible heat flux. During the late-snowmelt period, the amount of sublimation or evaporation in the snow surface was higher than that of deposition. Hence, latent heat flux turned negative (Table 2).

3.2 Temporal and spatial distribution of snow liquid water content before sunrise and after sunset

To describe the temporal and spatial distribution of snow liquid water content, three days (5 March, 31 March and 21 April 2010) in different snowmelt periods were selected as the typical distribution of snow liquid water. During the pre-snowmelt period (Fig. 4a), morning and afternoon snow liquid water were less than 1 %. Although liquid water content exceeded the liquid water-holding capacity except around 20 cm under the snow surface, no liquid water was drained from the snowpack. Thus, Anderson's formula may be suitable for all conditions. The maximum liquid water content was located at a depth ranging from 70 cm to 100 cm (the snow type was coarse snow) under the snow surface. With capillary effects ignored, according to Darcy's law describing liquid water movement in snow, the volume flux of liquid water is the largest in this range of depth and is bigger than at the snow bottom (the snow type was depth hoar). Hence, liquid water accumulated in this range. From the snow surface to 110 cm under

Discussion Paper | Discussion Paper | Discussion Paper | Discussion Paper |
TCD
6, 4137–4169, 2012
Changes in snow liquid water
H. Lu et al.

the snow surface, the average liquid water content increased from 0.31 % to 0.38 %. The average of snow liquid water content from 110 cm to 120 cm decreased, which may be attributed to measurement errors.

During the mid-snowmelt period (Fig. 4b), morning snow liquid water content was less than 0.5 % and increased with depth. The afternoon average liquid water content was 1.17 % and decreased with depth. From snow surface to 30 cm depth, liquid water content drastically changed from 0.36 % to 2.74 %. This result may be attributed to the low air temperature and the snow liquid water refreezing when the snow temperature was lower than 0 °C. The drastic variation from 30 cm to 40 cm depth may be ascribed to the depth range being not only a sink of moving liquid water from the upper layer, but also a liquid water source for the next layers. From 40 cm to the snow bottom, the diurnal change in liquid water content was small and stable (i.e., from 0.37 % to 0.43 %). The variation characteristics of snow liquid water content determined the snowmelt rates (Fig. 5a). The minimum and maximum snowmelt rates were 0.0186 and 0.038 $\text{kg}\,\text{m}^{-2}\,\text{h}^{-1}$, respectively, and then changed slightly.

During the late-snowmelt period (Fig. 4c), the morning snow liquid water content decreased with depth, and the minimum and maximum values were 0.59 % and 3.63 %, respectively. The average afternoon liquid water content was 4.77 %. The afternoon liquid water content decreased from the snow surface to a certain depth and then increased to the maximum value at the bottom of the snow. The liquid water content from the snow surface to 10 cm depth was large, which may be attributed to the sharp increase in net radiation. The snow porosity at the snow bottom (snow type is depth hoar) was larger than that at the other layers. Consequently, the liquid water content at the snow bottom was larger than that at the upper layers. The diurnal changes in the whole snow layer liquid water in this period were larger than the mid-snowmelt period. The variation trends of each layer were relative consistent. The snow temperature under 15 cm depth was not less than 0 °C all day, and the minimum air temperature increased with time. Thus, liquid water refreezing was not significant at this range. Figure 5b shows that the time of liquid water outflow was comparatively concentrated.

Thus, liquid water content movement is the most important factor for the distribution of snow liquid water content. The liquid water rapidly flowed to the next layer and discharged because the snow depth was far less than the mid-snowmelt period and the liquid water content exceeded water holding capacity.

3.3 Snow liquid water content in different weather conditions: rain or snow (ROS) events

ROS events change energy balance components, thereby causing changes in liquid water content and snowmelts. This study selected one event of snow and two events of rain and snow during different snowmelt periods to discuss the effect of ROS events. During a snowfall that occurred on 28 March, the precipitation was 33.3 mm, and the snowfall depth was 12 cm. Figure 6 shows that the net radiation during snowfall was far less than that before snowfall and that the sensible heat flux was negative. Thus, the afternoon liquid water content on 28 March was less than that on 27 March, and the distribution was different, especially from the snow surface to 20 cm depth (Fig. 7). The net radiation and sensible heat flux after snowfall were less than those before snowfall. This finding may be attributed to the high snow albedo and "dry-cold" weather condition. Therefore, the average liquid water content of the whole snow layer after snowfall was less than that before and during snowfall. In addition, the diurnal variation also decreased. The distribution of liquid water content was in accordance with the typical distribution (Fig. 4b). The snowmelt rate decreased during and after snowfall because of the changes in liquid water content (Fig. 6).

A rainfall occurred from 23:00, 3 April to 23:00, 4 April, with a precipitation of 16.1 mm Rain and snow occurred from 09:00, 5 April to 23:00, 5 April, with a precipitation of 12.6 mm and a snowfall depth of 3 cm. The total energy during the ROS period was less that during the non-ROS period. Net radiation and sensible heat flux during the ROS period were less than those during the non-ROS period, whereas latent heat flux during the ROS period was larger than that during the non-ROS period. However, the variation trend and distribution of liquid water content were different only from the snowfall event (Fig. 7). On 4 April, the energy supplied by precipitation was 102.82 MJ, which was much higher than other heat fluxes. Thus, the average liquid water content was 2.12 %, and the snowmelt rate did not decrease. On 5 April, the energy supplied by precipitation was −3.76 MJ. However, the difference between snow liquid water content and distribution with non-ROS period was not significant. This finding may be attributed to the rainfall-induced increase in the heat flux and liquid water in the snowpack. As an insulator, newly formed snow protects the temperature of the old snow from decreasing. Thus, the morning liquid water content on 5 March and 6 March was larger than that during the non-ROS period.

An ROS event occurred from 09:00, 17 April to 11:00, 18 April, with a precipitation of 19.8 mm and a snow depth decrease of 1 cm. A snowfall occurred from 23:00, 18 April to 21:00, 19 April, with a precipitation of 20.7 mm and a snowfall depth of 12 cm. During the ROS period, net radiation decreased and the energy supplied by precipitation was 35.4 MJ. However, the afternoon liquid water content on 17 April was less than that during the non-ROS period (Figs. 4c and 11), and the snowmelt rate did not increase sharply (Fig. 10). The liquid water from rain was rapidly discharged. Hence, most part of the energy supplied by precipitation cannot exchange with snow. From 11:00 to 20:00, 18 April was a clear day, and the characteristic of liquid water was in accordance with that during the non-ROS period (Fig. 4c). On 19 April, net radiation and sensible heat flux were negative and the energy supplied by precipitation was −4.26 MJ. Thus, the liquid water content decreased, especially from the snow surface to 20 cm depth. At the bottom of the snow, the ROS event caused significant changes in liquid water, showing a difference from the mid-snowmelt period.

3.4 Regression equation of snow liquid water content

The changes in snow depth were significant during the snowmelt period, revealing information regarding temperature, radiation, liquid water movement and so on. Snow liquid water content mainly depended on energy balance, liquid water movement and ROS event. Thus, snow depth is a good index to indicate changes in liquid water

TCD
6, 4137–4169, 2012

content. Snow liquid water can be fitted with an exponential function:

$$W_{vol} = 18.892e^{-0.028h} \quad (16)$$

where W_{vol} is the snow liquid water content (%) and h is the snow depth (cm). The fit has an R^2 equal to 0.86, and predicted values of W_{vol} have an uncertainty of 0.076 %.

However, the characteristics of snow depth differ annually. Thus, the function may not be suitable for other years. Therefore, the regression function of liquid water should be built based on the physical mechanism and processes. Radiation, wind, and snow surface temperature cannot be easily obtained during field measurements. Thus, air temperature is the most suitable parameter for regression equation. Snow liquid water depends on the air temperature of the current day as well as that of the previous days. Snow liquid water content exponentially increased with prior moving average air temperature (Fig. 12) and can be fitted using the following equation:

$$W_{vol} = 1.8433e^{0.2478T_{ma}} \quad (17)$$

where W_{vol} is the snow liquid water content (%) and T_{ma} is the prior moving average air temperature (°C). The span is 7, according to the correlation between liquid water content and average air temperature, and the weight values were 0.15, 0.1, 0.05, 0.05, 0.15, 0.2, and 0.3. The fit has an R^2 of 0.85, and predicted values of W_{vol} have an uncertainty of 0.16 %.

4 Conclusions

The average water content of the whole layer exponentially increased with time and average air temperature. Snow liquid water content can be calculated by a regression function of prior moving average temperature. According to the liquid water content, the snowmelt period can be divided into three stages (pre-snowmelt period: $0.3\% \le W_{vol} < 1\%$, mid-snowmelt period: $1\% \le W_{vol} < 2.5\%$, and late-snowmelt period: $W_{vol} \ge 2.5\%$).

During the pre-snowmelt period, air temperature gradually increased and net radiation was small. Sensible heat flux was the most important part of total energy. Snow liquid water content and the variation were relatively smaller. The liquid water moved from the upper layer to the next layers and accumulated in the coarse snow layer. The snowpack did not have liquid water discharged. Thus, the snow period was in the mature stage.

During the mid-snowmelt period, net radiation and latent heat flux were the major parts of the total energy because of the increase in astronomical radiation and specific humidity. From the snow surface to 30 cm depth, the liquid water was refreezing in the evening. Thus, the daily variation in liquid water content was drastic. The liquid water content from 40 cm to the snow bottom was smaller than that in the upper layers. The variation was also less and was more stable. During this period, liquid water was discharged from the snowpack. The weather process (ROS) was frequent during this period. Snow liquid water content and the variation decreased during snowfall and the following one to two days. The total energy and liquid water increased because of precipitation (ROS event). With the old snow covered by newly formed snow, the distribution of liquid water content from the snow surface to 30 cm depth was in accordance during the non-ROS period (afternoon). The diurnal change in liquid water content was smaller on the ROS day than on the clear day.

During the late-snowmelt period, the proportion of net radiation that occupied total energy was larger than 70 % with astronomical radiation increasing and snow albedo decreasing. Moreover, the latent heat flux was negative. The distribution and variation of every snow layer showed a uniform trend. Liquid water was moved to the next layer and was rapidly discharged from the snowpack. The effect of ROS event on liquid water content during the late-snowmelt period was different from that during the mid-snowmelt period. Significant changes in liquid water content were noted from the snow surface to 30 cm depth and at the bottom of the snowpack. The ROS event affected snow liquid water content during the ROS period only, which was different from the mid-snowmelt period.

TCD
6, 4137–4169, 2012

Acknowledgements. The research presented in this article was jointly funded by National Natural Science Foundation of China (41171066); the Western Light Project (RCPY200902) of the Chinese Academy of Sciences.

References

Anderson, E.: A point energy and mass balance model of a snow cover. Office of Hydrology, National Weather Service, Silver Spring, Maryland, NOAA Technical Report NWS 19, 1976.

Andreas, E.: Parameterizing scalar transfer over snow and ice: a review, J. Hydrometeorol., 3, 417–32, 2002.

Boon, S.: Snow ablation energy balance in a dead forest stand, Hydrol. Process., 23, 2600–2610, 2009.

Boyne, H. and Fisk, D.: A comparison of snow cover liquid water measurement techniques, Water Resour. Res., 23, 1833–1836, 1987.

Brun, B., Martin, E., Simon, V., Gendre, C., and Coleod, C.: An energy and mass model of snow cover suitable for operational avalanche forecasting, J. Glaciol., 35, 333–342, 1989.

Che, Z. X., Jin, M., Zhang, X. L., Zhang, H., Niu, Y., and Dong, X. L.: Effect of vegetation type on the ablation of snow cover in the Qilian Mountains, J. Glaciol. Geocryol., 30, 24–28, 2008 (in Chinese).

Chen, X., Wei, W. S., and Liu, M. Z.: Characteristics of temperature variation in seasonal snow in the Western Tianshan Mountains, China, Meteorol. Appl., doi:10.1002/met.1308, 2012.

Colbeck, S.: A theory of water percolation in snow, J. Glaciol., 11, 369–385, 1972.

Colbeck, S.: Theory of particle coarsening with a log-normal distribution, Acta Metall. Mater, 35, 1583–1588, 1987.

Colbeck, S. and Anderson, E.: The permeability of a melting snow covers, Water Resour. Res., 18, 904–908, 1982.

Conway, H. and Raymond, C.: Snow stability during rain, J. Glaciol., 39, 635–642, 1993.

Davis, R., Dozier, J., LaChapelle, E., and Peral, R.: Field and laboratory measurement of snow liquid water by dilution, Water Resour. Res., 21, 1415–1420, 1985.

Donoth, A.: An electronic device for long-term snow wetness recording, Ann. Glaciol., 19, 104–106, 1994.

Dozier, J. and Painter, T.: Multispectral and hyperspectral remote sensing of alpine snow properties, Annu. Rev. Earth Pl. Sc., 32, 113–126, 2004.
Fisk, D.: Method of measuring liquid water mass fraction of snow by alcohol solution, J. Glaciol., 32, 538–540, 1986.
Jin, J., Gao, X., Sorooshian, S., Yang, Z. L., Bales, R., Dickinson, R. E., Sun, S. F., and Wu, G. X.: One-dimensional snow water and energy balance model for vegetated surfaces, Hydrol. Process., 13, 2467–82, 1999.
Jones, E. and Rango, A.: A comparison of centrifuge and freezing calorimeter methods for measuring free water in snow, Report NBSIR 79-1604, Boulder, CO, National Bureau of Standards, 1979.
Jones, E., Rango, A., and Howell, S.: Snowpack liquid water distributions using freezing calorimetry, Nord. Hydrol., 14, 113–126, 1983.
Kattelmann, R. and Dozier, J.: Observation of snowpack ripening in the Sierra Nevada, California, USA, J. Glaciol., 45, 409–416, 1999.
Kawashima, K., Endo, T., and Takeuchi, Y.: A portable calorimeter for measuring liquid-water content of wet snow, Ann. Glaciol., 26, 103–106, 1998.
LaChapelle, E.: Properties of snow, prepared for Hydrologic Systems course presented by College of Forest Resource, 17–18 Nov., University of Washington, Seattle, 21 pp., 1969.
Lehua, P., Warrick, A., and Wierenga, P.: Downward water flow through sloping layers in the vadose zone: time-dependence and effect of slope length, J. Hydrol., 199, 36–52, 1997.
Li, Z. J., Zhao, Z. Q., Feng, E. M., Cheng, B., and Lu, P.: Time-space distribution of water content in the snow on Arctic sea ice surface in summer, Adv. Water Sci., 18, 24–28, 2007 (in Chinese).
Lzumi, K.: Effects of solar radiation on the formation of weak wet snow, Ann. Glaciol., 13, 120–123, 1989.
Male, D. and Gray, D.: Handbook of Snow, Principles, Processes, Management and Use, Pergammon Press, Toronto, 360–436, 1981.
Marsh, P.: Grain growth in a wet arctic snow cover, Cold Reg. Sci. Technol., 14, 23–31, 1987.
Mitterer, C., Mott, R., and Schweizer, J.: Observations and analysis of two wet-snow avalanche cycles, in: Proceeding of International Snow Sciences Workshop, WSL Institute for Snow and Avalanche Research SLF, Davos, Switzerland, 262–266, 2009.
Moore, R.: A comparison of the snowmelt energy budgets in two alpine basins, Meteorol. Atmos. Phys., 33, 1–10, 1983.

Morris, E.: Field measurement of the liquid-water content of snow, J. Glaciol., 27, 175–178, 1981.
Niang, M., Bernier, M., Stacheder, M., Brandelik, A., and Bochove, E.: Influence of snow temperature interpolation algorithm and dielectric mixing-model coefficient on density and liquid water content determination in a cold seasonal snow pack, Sensing and Imaging, 7, 1–22, 2006.
Schneebeli, M., Coleiu, C., Touvier, F., and Lesaffre, B.: Measurement of density and wetness in snow using time-domain reflectometry, Ann. Glaciol., 26, 69–72, 1998.
Sihvola, A. and Tiuri, M.: Snow Fork for field determination of density and wetness profiles of a snow pack, IEEE T. Geosci. Remote, GE-24, 717–721, 1986.
Singh, A.: An investigation of the thermal conductivity of snow, J. Glaciol., 45, 346–351, 1999.
Techel, F. and Pielmeier, C.: Point observations of liquid water content in wet snow – investigating methodical, spatial and temporal aspects, The Cryosphere, 5, 405–418, doi:10.5194/tc-5-405-2011, 2011.
Trautman, S., Lutz, E., Birkeland, K., and Custer, S.: Relating wet loose snow avalanching to surficial shear strength, in: Proceeding International Snow Science Workshop 2006, Telluride, CO, USA, 71–78, 2006.
Verseghy, D.: CLASS-A Canadian land surface scheme for GCMs, I. Soil model, Int. J. Climatol., 1, 111–133, 1991.
Wakahama, G.: The metamorphism of wet snow, Low temperature Science Series, 23, 51–66, 1956.
Wei, W. S., Qin, D. H., and Liu, M. Z.: Properties and structures of the seasonal snow cover in the continental regions of China, Ann. Glaciol., 32, 93–101, 2001.
Zhang, Z. Z.: Preliminary analyses of the release causes for wet-snow avalanches in the Kunas Valley, Tianshan Mountains, J. Glaciol. Geocryol., 8, 403–407, 1986 (in Chinese).
Zhou, S. Q., Hashimoto, S., Nakawo, M., and Narita, H.: Mathematical modeling of water percolation in snow, J. Hydraul. Eng., 1, 6–10, 2001 (in Chinese).

TCD
6, 4137–4169, 2012

Changes in snow liquid water

H. Lu et al.

Table 1. Correlation between the whole layer average water content and the different temperature indices.

	Daily average air temperature	Maximum air temperature	Minimum air temperature	Accumulated air temperature
Snow liquid water content	0.694*	0.644*	0.549*	0.731*

* Has passed the significance test of 0.01.

Table 2. Proportion of different heat flux occupied total energy (not including energy supplied by precipitation).

	Net radiation	Sensible heat flux	Latent heat flux
Pre-snowmelt period	18.7 %	59.3 %	22.0 %
Mid-snowmelt period	51.2 %	12.1 %	36.7 %
Late-snowmelt period	71.4 %	29.3 %	−0.7 %
All snowmelt periods	48.3 %	27.3 %	24.4 %

TCD
6, 4137–4169, 2012

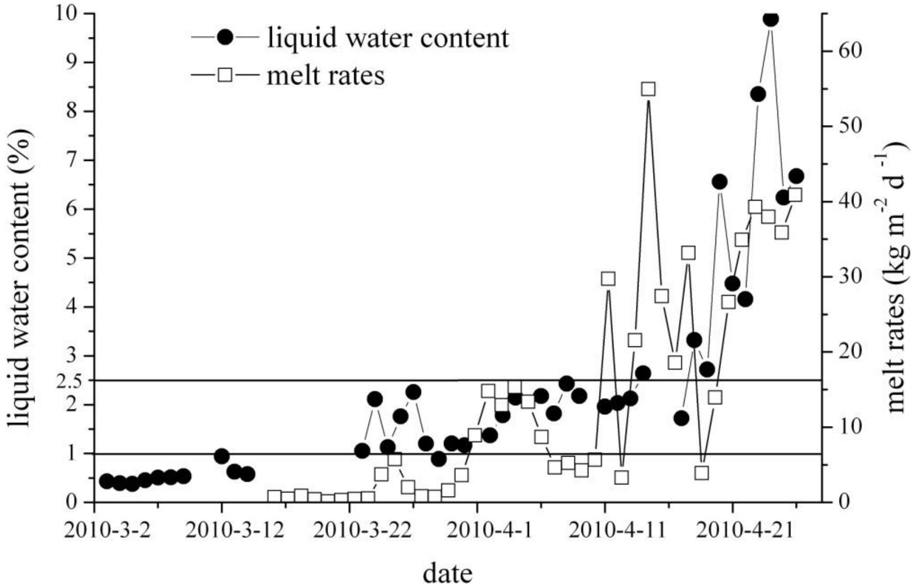

Fig. 1. Variation trend of liquid water content in the whole snow layer and melt rates.

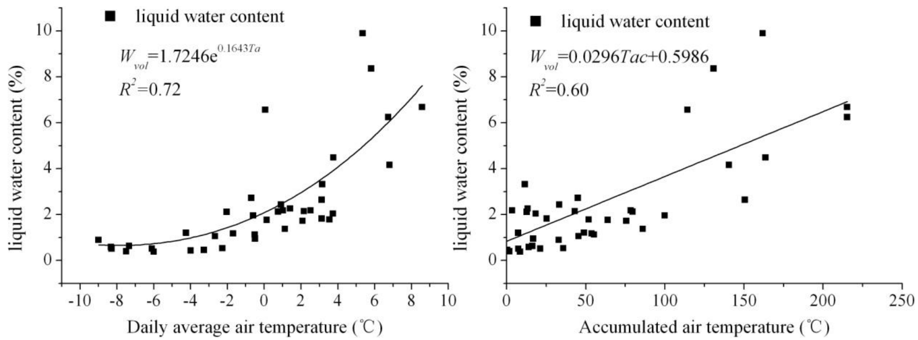

Fig. 2. Relationship between the different temperature indices and liquid water content: **(a)** snow liquid water content vs. daily average air temperature, **(b)** snow liquid water content vs. accumulated air temperature.

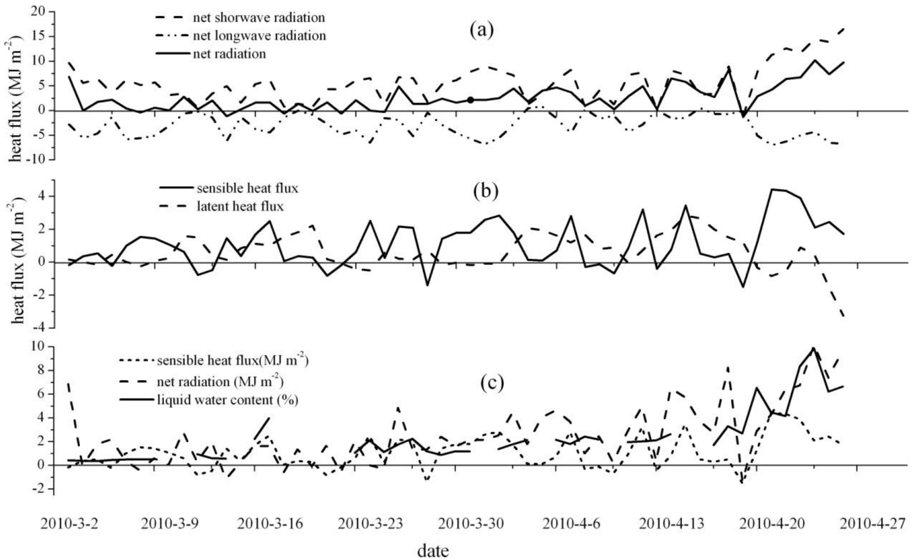

Fig. 3. Sensible heat flux, latent heat flux, and radiation during the snowmelt period: **(a)** the variation of net shortwave radiation, net longwave radiation and net radiation, **(b)** the variation of sensible heat flux and latent heat flux, **(c)** the variation of sensible heat flux, net radiation and snow liquid water content.

TCD
6, 4137–4169, 2012

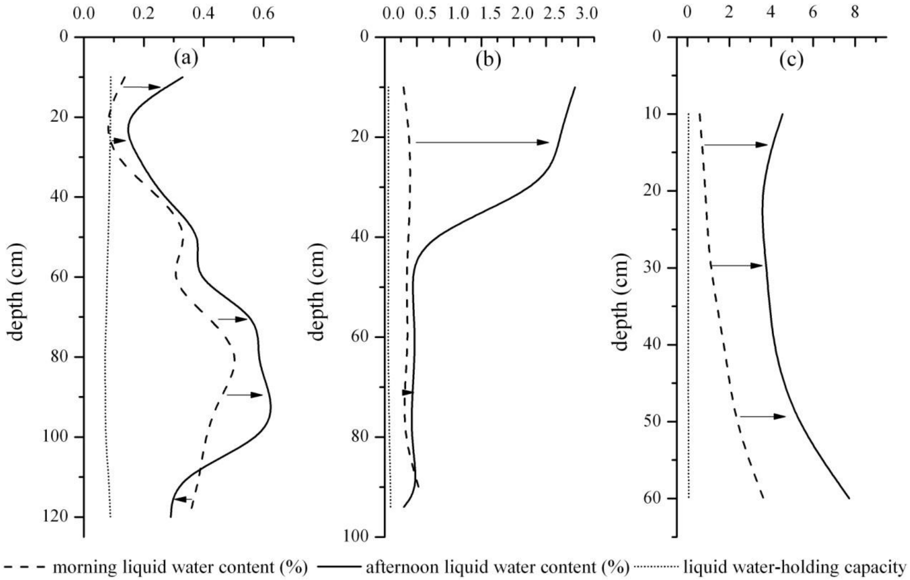

Fig. 4. Difference between morning and afternoon liquid water content and liquid water-holding capacity: **(a)** pre-snowmelt period, **(b)** during mid-snowmelt period, **(c)** late-snowmelt period.

TCD
6, 4137–4169, 2012

Title Page
Abstract | Introduction
Conclusions | References
Tables | Figures
◀I | ▶I
◀ | ▶
Back | Close
Full Screen / Esc
Printer-friendly Version
Interactive Discussion

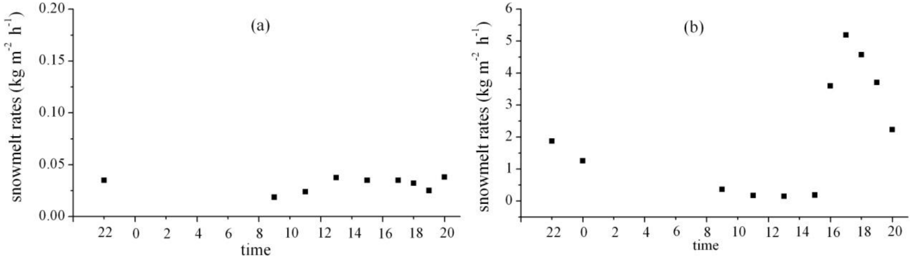

Fig. 5. Diurnal changes in snowmelt rates during the different snowmelt periods: **(a)** mid-snowmelt period, **(b)** late-snowmelt period.

TCD
6, 4137–4169, 2012

Changes in snow liquid water

H. Lu et al.

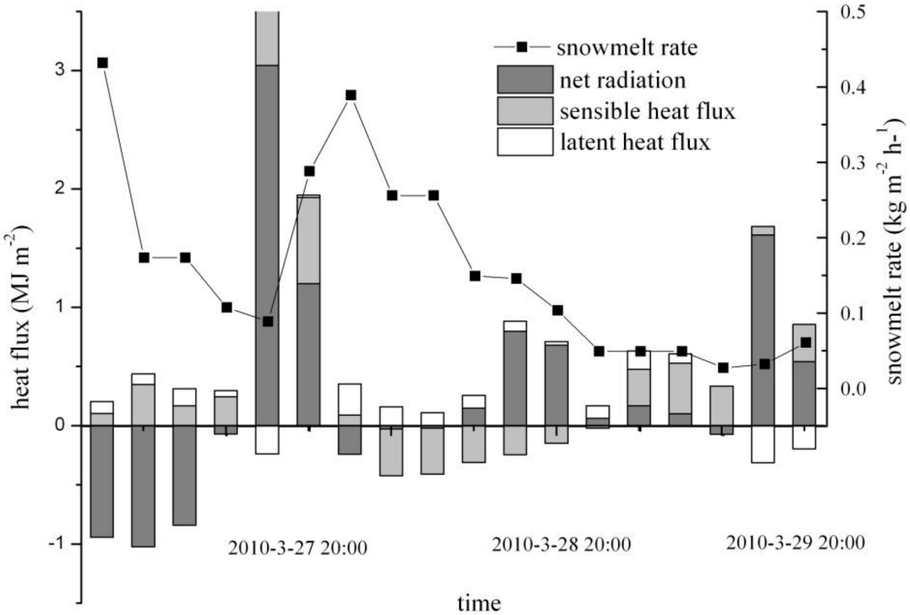

Fig. 6. Energy balance components of the snow event on 28 March (4 h time step).

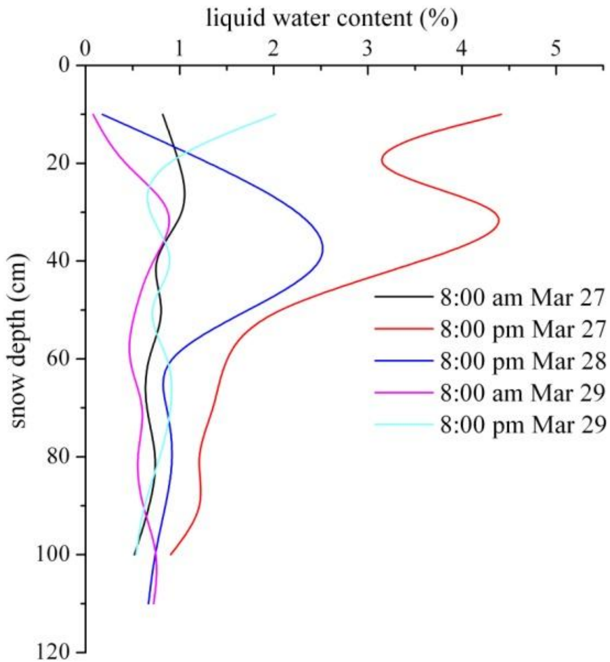

Fig. 7. Changes in liquid water content from 27 March to 29 March.

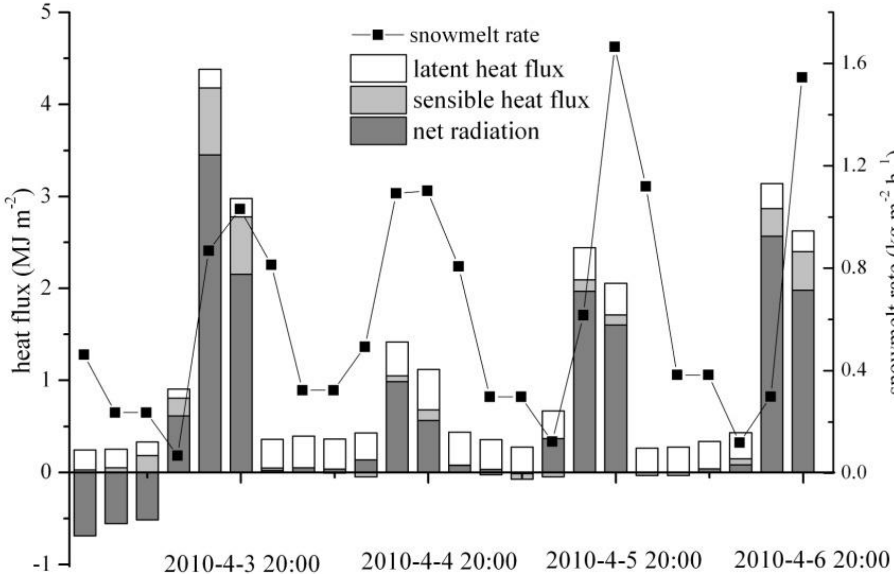

Fig. 8. Energy balance components for the ROS event from 4 April to 5 April (4 h time step).

TCD
6, 4137–4169, 2012
Changes in snow liquid water
H. Lu et al.

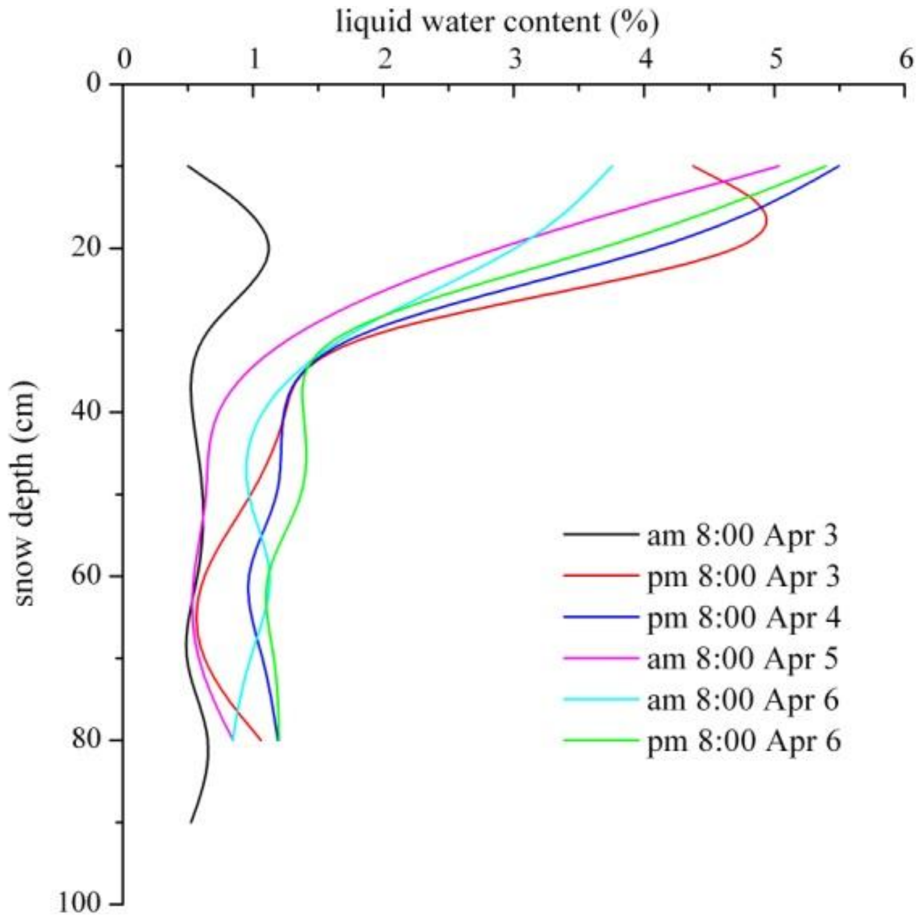

Fig. 9. Changes in liquid water content from 3 April to 6 April.

TCD
6, 4137–4169, 2012

Changes in snow liquid water

H. Lu et al.

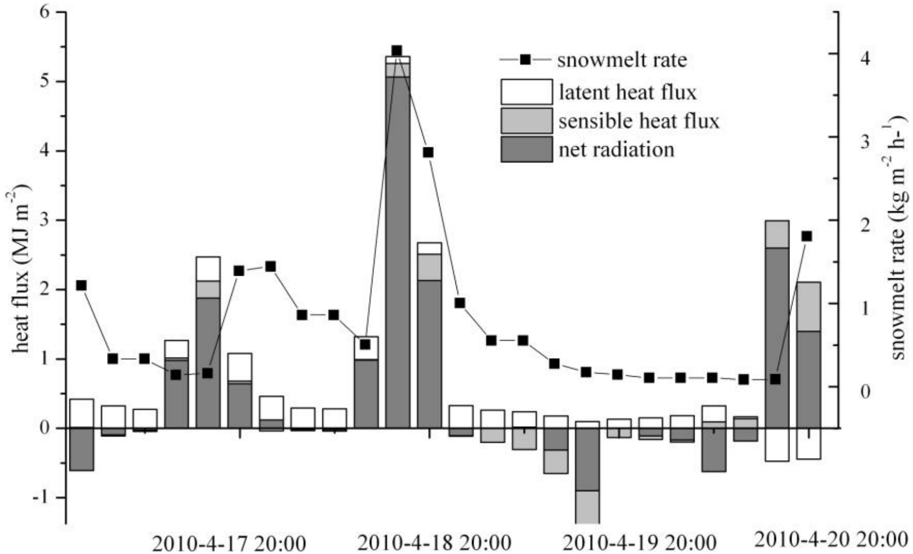

Fig. 10. Energy balance components for the rain and snow event from 17 April to 20 April (4 h time step).

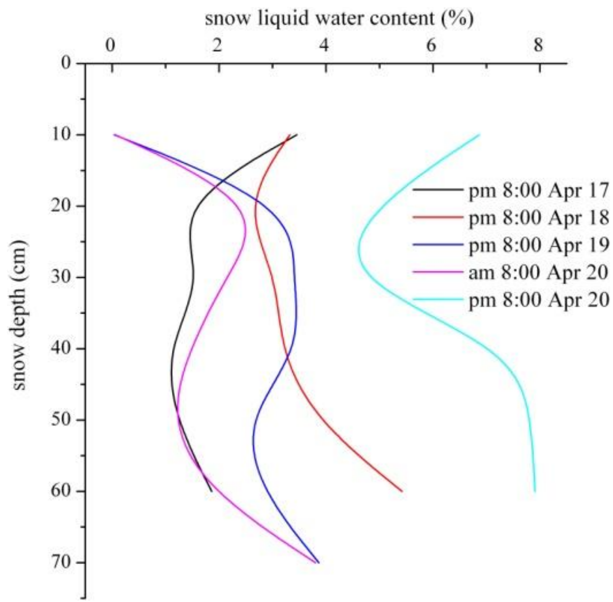

Fig. 11. Changes in liquid water content from 17 April to 20 April.

TCD
6, 4137–4169, 2012

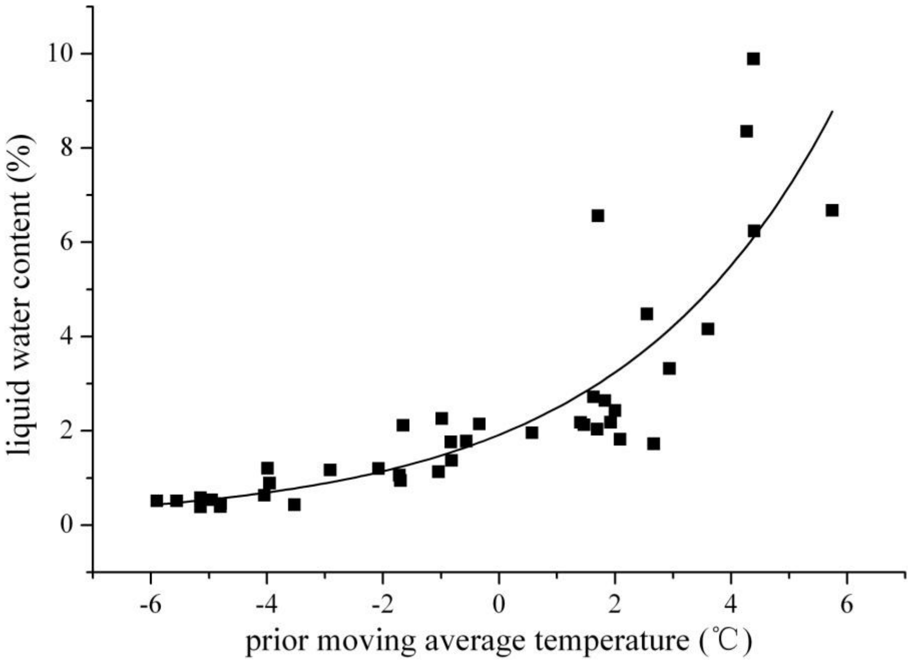

Fig. 12. Relationship between prior moving air temperature and liquid water content.